Journal of Electroanalytical Chemistry 796 (2017) 57–65

Contents lists available at ScienceDirect

Journal of Electroanalytical Chemistry

journal homepage: www.elsevier.com/locate/jelechem

Electrodeposition and characterization of Ni-Mo alloy as an electrocatalyst for alkaline water electrolysis

Sandhya Shetty, M. Mohamed Jaffer Sadiq, D. Krishna Bhat, A. Chitharanjan Hegde*

Department of Chemistry, National Institute of Technology Karnataka, Surathkal, Srinivasnagar 575025, India

ARTICLE INFO

Keywords:
Ni-Mo alloy
Corrosion
Water splitting
HER
OER study

ABSTRACT

This work details the efficiency of Ni-Mo alloy as an electrode for water splitting application through electrodeposition method. Nano-crystalline Ni-Mo alloy coatings were deposited in the current density (c.d.) range of 1.0–4.0 A dm^{-2} on a copper substrate, and were investigated for their deposit characters, and their electrocatalytic behaviours in 1.0 M KOH solution. The electrocatalytic behaviour of the coatings, in terms of their hydrogen evolution reaction (HER) and oxygen evolution reaction (OER), were evaluated by electrochemical methods, like cyclic voltammetry (CV) and chronopotentiometry (CP). Experimental results revealed that Ni-Mo alloy electrodeposited at 1.0 A dm^{-2} (38.3 wt% Mo) and 4.0 A dm^{-2} (33.2 wt% Mo) shows the highest electrocatalytic tendency for HER and OER, respectively. The corrosion behaviour of Ni-Mo alloy coated at 4.0 A dm^{-2} is found to be the most corrosion resistant in the same alkaline medium, compared to other coatings. The highest electrocatalytic activity of Ni-Mo alloy deposit for both HER and OER, depending on deposition c.d. was attributed to their composition (in terms of Ni and Mo content), structure and surface morphology; supported by EDXA, XRD, SEM and AFM analyses. The experimental study demonstrated that Ni-Mo alloy coatings follow Volmer-Tafel type of mechanism for HER, testified by Tafel slope analyses.

1. Introduction

Hydrogen, the most abundant element on earth, is the cleanest and an ideal fuel. Hence, it is considered as the efficient fuel in the future [1]. An important method employed for the production of hydrogen is water electrolysis. However, this method happens to be expensive due to its high-energy consumption. In recent years, considerable efforts are made in studying cathodic electrode materials being able to drastically lower hydrogen over-potential and to increase the production of hydrogen gas. Alkaline solutions are commonly used in water electrolysis, and main properties that the electrodes are considered to have a large active surface area, long-term electrochemical stability, good electrical conductivity, low hydrogen overpotential, excellent electrocatalytic activity and a high resistance to corrosion [2]. But, it is well known that except for noble metals, other less-noble metals show much less activity for HER. In this direction, several 3d - transition metal-based alloys have been tried, mostly binary alloys of Ni- or Co- and some other transition metals (Mo, Zr, Fe, etc.). The combination of any two transition metals could indeed enhance the HER electrocatalytic activity compared to their individual activities, explained by well-known synergetic effect [3]. Further, the literature reveals that electrocatalytic activity of electrode materials can be increased substantially by introducing a foreign dopant into an electrode possessing high surface areas, or better electroactive sites. Hence, Ni and its alloys are traditionally being used as the material of choice for electrodes to catalyse water electrolysis for both HER [4,5] and oxygen evolution reaction (OER) [6–8]. Ni is commonly used as a reference for comparison with new electrocatalysts for the OER [9,10], due to the fact that OER typically takes place on the surface of metal oxides or hydroxides. Studies on Ni oxides and hydroxides, when combined with Co, Mo, and Fe, produced by several chemical, thermal and electrochemical routes [10–12] and high-energy ball mill method [13], have been carried out.

Among Ni-based alloys, Ni-Mo alloy is well known for its use as cathode material for HER by water electrolysis [14]. Arul Raj and Venkatesan [15] exhibited an improved electrocatalytic effect of electrodeposited Ni-Mo alloys for HER than that of Ni and other Ni-based binary alloys such as Ni-Co, Ni-W, Ni-Fe, and Ni-Cr. It was also that electrodeposited Ni-Mo alloy coatings exhibit good anticorrosive behaviour, mechanical and thermal stability by following induced codeposition mechanism [16]. Many reported documents revealed that an effective nano-crystalline Ni-Mo electrocatalyst can be developed by electrodeposition method. The electrolytic synthesis of Ni-Mo alloy coating has advantages over other methods, like a deposit of desired

* Corresponding author.
E-mail address: achegde@nitk.ac.in (A.C. Hegde).

http://dx.doi.org/10.1016/j.jelechem.2017.05.002
Received 26 January 2017; Received in revised form 21 April 2017; Accepted 2 May 2017
Available online 03 May 2017

composition, porosity, low-temperature growth could be produced. With this method, there also is a possibility to control the thickness, morphology, and phase structure of the coating by adjusting certain electrical parameters and the composition of electrolytes [17].

In this regard, the present paper reports the experimental results of the examination on electrodeposition and characterization of Ni-Mo alloy for water electrolysis i.e., (HER and OER) in the alkaline medium. The paper is divided into three parts. The first part details on the chemical, structural and morphological characterization of Ni-Mo coatings deposited at varying of current densities (c.d.). The second and third part details on the electrocatalytic behaviour of Ni-Mo coatings developed at different c.d. for HER and OER, respectively through cyclic voltammetry (CV) and chronopotentiometry (CP) techniques. The optimal conditions of deposition of Ni-Mo alloy for highest HER and OER have been proposed, and results are discussed.

2. Material and methods

2.1. Electrodeposition of Ni-Mo alloy coatings

The Ni-Mo electrolytic bath has been prepared from analytical grade reagents (Merck, India) using double distilled water. Here, nickel sulphate ($NiSO_4{\cdot}6H_2O$) and sodium molybdate (Na_2MoO_4) were used as a source of metal salts and tri-sodium citrate ($Na_3C_6H_5O_7$) as complexing salt. The optimal bath composition and operating parameters for deposition of hard adherent Ni-Mo alloy coating were arrived by standard Hull cell method [18]. The pH of the bath was maintained at 9.5 (Systronics, μ pH Systems 362) by using either dil. NH_4OH or H_2SO_4, depending on requirement. The electrolyte was filtered using Whatmann-40 filter paper before each deposition, to remove suspended anodic impurities and other insoluble particles. Bath composition and operating parameters of the optimized bath is shown in Table 1.

Ni-Mo alloy coatings were deposited on copper plates, and on a cross-sectional area of the copper rod (both having same specifications), depending on the requirement for characterization. For surface morphology, composition and X-ray diffraction (XRD) analyses, Ni-Mo alloy coatings were carried out on known surface area (2.5 cm × 2.5 cm) of copper plates (7.5 cm × 2.5 cm × 0.2 cm) in 200 mL capacity cubic cell (made of PVC material), by covering the remaining region of the plate with cellophane tape. All electrochemical and electrocatalytic study of Ni-Mo alloy coatings were carried out by depositing it onto the cross-sectional surface area of a copper rod (1.0 cm^2), in a customized glass cell as shown in Fig. 1.

The copper substrate was ground to the mirror finish, using grinding wheels of varying grade emery mops, and then degreased using trichloroethylene. It was then electro-cleaned and pickled in 0.5 M HNO_3 to activate the surface prior to deposition and then rinsed with distilled water. Copper substrate was used as a cathode in the electrochemical cell, and pure nickel plate of same exposed surface area as an anode; maintaining a distance of 5 cm from each other. All electrodeposition was carried out under the galvanostatic condition, from the optimal bath (refer Table 1), under the condition of constant agitation using DC Power Analyzer (Agilent N6705A, USA), as the power source. Electrodepositions were carried out at different c.d.

Table 1
The composition and deposition conditions of the optimized Ni-Mo bath.

Bath constituents	Amount (g L^{-1})	Operating parameters
$NiSO_4{\cdot}6H_2O$	18	Anode: pure Ni plate
Na_2MoO_4	48	Cathode: copper
$Na_3C_6H_5O_7$	105	pH: 9.5
		Temperature: 303 K
		Deposition time: 10 min
		Current density: 1.0–4.0 A dm^{-2}

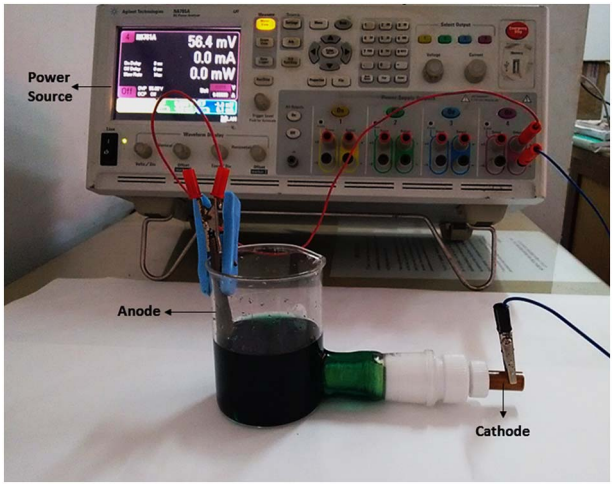

Fig. 1. Customized glass cell used for electrodeposition of Ni-Mo alloy on a cross-sectional surface area of a copper rod for studying its electrocatalytic behaviour.

(1.0–4.0 A dm^{-2}) for a constant duration (600 s) to compare their relative performance. Finally, the coatings after the deposition were rinsed several times with distilled water, later dried in hot air, and then desiccated until further testing.

2.2. Experimental set up

Electrocatalytic study of Ni-Mo alloy has been carried out using a three-electrode tubular glass cell (customized), shown schematically in Fig. 2. This experimental setup enabled the quantitative evaluation of the electrocatalytic behaviour of Ni-Mo alloy deposited under different conditions of c.d. The customized cell is designed to collect the liberated H_2 and O_2 gas when the electrode is subjected to cathodic and anodic polarization, respectively. The platinum electrode of 1.0 cm^2 surface area is used as a counter electrode placed at one end of the tube and electrodeposited Ni-Mo alloy at another end, which serves as a working electrode. Saturated calomel electrode (SCE) is used as a reference electrode and its connection is established through Luggin's capillary with Agar-KCl salt bridge which eliminates the error due to *iR* drop. All potentials reported in this work were converted from the SCE to the RHE scale using ((RHE) = E(SCE) + 1.030 V) in 1.0 M KOH. The cell is fitted with graduated tubes (burette), which collects the volume of liberated gas (hydrogen and oxygen) displacing the solution, whose volume could be easily read. This arrangement helps in evaluating the electrocatalytic efficiency of Ni-Mo alloy by measuring the amount of H_2 and O_2 generated at anode and cathode, respectively.

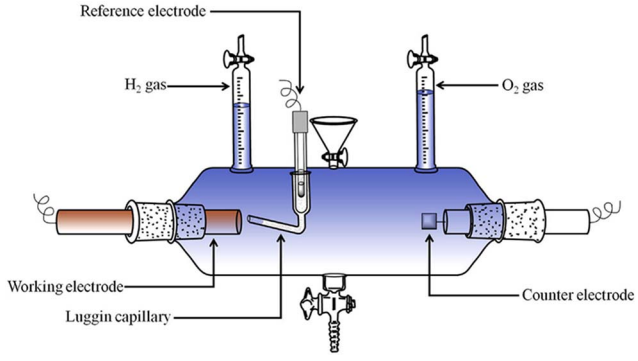

Fig. 2. Experimental set up used for quantitative evaluation of the electrocatalytic performance of Ni-Mo alloy coatings.

2.3. Electrochemical measurements

The electrocatalytic activity of Ni-Mo deposits developed at different c.d. (for both HER and OER) were evaluated by subjecting them to cyclic voltammetry (CV) and chronopotentiometry (CP) study in 1.0 M KOH medium, using electrochemical workstation (IVIUM VERTEX, Netherlands). Potentiodynamic polarization study was carried out by polarizing the test electrode by subjecting it to a potential drift − 250 mV cathodically, and + 250 mV anodically relative to the OCP at a scan rate of 1.0 mV s^{-1}. The potentiodynamic Tafel curves were simultaneously plotted, and through Tafel extrapolation method, the polarization parameters like corrosion potential (E_{corr}), corrosion current density (i_{corr}), corrosion rate (CR) and cathodic slope (β_c) were deduced.

The corrosion rate was calculated using the following equation [19]:

$$CR\ (mm\ y^{-1}) = \frac{K \times i_{corr} \times EW}{\rho} \quad (1)$$

where, constant K = 0.00327, ρ = density of the corroding material, EW = equivalent weight of the deposited alloy. Corrosion parameters were used to evaluate the corrosion stability of Ni-Mo alloy in alkaline 1.0 KOH medium, and the cathodic slopes, β_c were used in understanding the mechanism pathway for HER.

2.4. Characterization of Ni-Mo coatings

Surface morphology of coatings was examined using scanning electron microscopy (SEM) (EVO 18, Carl Zeiss, Germany). The composition of coatings was studied by Energy Dispersive X-ray (EDX) technique, interfaced with SEM instrument. Structural change of Ni-Mo alloys coatings due to the effect of c.d. was analysed by X-ray diffraction (XRD) study (Rigaku Miniflex 600), using Cu Kα (λ = 1.5406 Å) radiation, in continuous scan mode at a scan rate of 2° min^{-1}. The structural analyses were done using the computer software (PANalytical X'Pert Highscore Plus). Atomic force microscopy (AFM) measurements were carried out using Innova SPM Atomic Force Microscope. The surface of the alloy coatings was mapped in tapping mode, using antimony doped silicon cantilever having a force constant in the range of 20–80 N m^{-1}. The surface roughness of the coatings was expressed in terms of their average roughness.

3. Results and discussion

3.1. Characterization of Ni-Mo alloy coatings

Electrodeposition of Ni-Mo alloy coatings was carried out at different c.d. (from 1.0 to 4.0 A dm^{-2}) using the optimal bath (Table 1). Though molybdenum (Mo) is quite an electro active metal, it cannot be deposited by itself from its electrolytic bath but can only be deposited in presence of another metal, through induced co-deposition [20]. Accordingly, in the electrodeposition of Ni-Mo alloy, Ni stimulates the deposition process and is called the inducing metal, and Mo is called the reluctant metal. Generally, it has been observed that in induced codeposition there is no consistent trend in the reluctant metal content in the deposit with c.d. i.e. variations in properties of electrodeposited Ni-Mo alloy coatings with c.d. is quite unpredictable, and hence the scope for studying the structure-property relationship of Ni-Mo alloy is quite vagarious. Therefore, in the present study Ni-Mo alloy coatings electrodeposited at different c.d. were first characterized for their basic properties, like morphology, composition, phase structure and corrosion resistance.

3.1.1. Surface analysis

The surface morphology of Ni-Mo alloy coatings, deposited at different c.d. is shown in Fig. 3. It may be observed that the coatings deposited at 1.0 A dm^{-2} and 2.0 A dm^{-2} found to exhibit a nodular structure as shown in Fig. 3(a) and (b), respectively. Then, as the c.d. increased the size of nodules increased, but fewer in numbers making the surface smoother and uniform as may be seen in Fig. 3(c) and (d). Further, Ni-Mo alloy coatings deposited at high c.d. were characterized by some pin holes by attributed to the evolution of hydrogen during codeposition [21]. Thus, from SEM micrographs of Ni-Mo alloy coatings, it may be inferred that surface morphology of the coatings bears a close relationship with applied c.d. Further, from the data shown in Table 2, it may be noted that applied c.d. has a strong influence on the composition of coatings. It may be further noted that towards lower c.d. the wt% of Mo is high. Hence the surface is characterized by a nodular coarse-grained structure. This increased Ni content at high c.d. range is responsible for increased electrocatalytic activity of the coatings for OER, as will be discussed.

3.1.2. AFM study

The AFM is a powerful means to characterize the microstructure of the coatings, in terms of their average roughness. Accordingly, a three-dimensional AFM image of the Ni-Mo alloy coatings at 1.0 A dm^{-2} and 4.0 A dm^{-2} (only extreme representatives) have been taken, and are shown in Fig. 4a and b, respectively. A clear difference in the surface roughness of the coatings was observed, as the c.d. is increased from 1.0 A dm^{-2} to 4.0 A dm^{-2}. Experimental data analysis revealed that the average roughness of coatings at 1.0 A dm^{-2} (Fig. 4a) and 4.0 A dm^{-2} (Fig. 4b) are, respectively 17.0 and 9.11 nm. The increased surface roughness, and hence the active surface area of Ni-Mo alloy coatings at 1.0 A dm^{-2} is in compliance with is SEM micrograph as shown in Fig. 3.

3.1.3. EDX analysis

The compositional analyses of Ni-Mo alloys deposited at various applied c.d. were carried out by EDX method. A strong influence of the c.d. on Mo content of the coating was found. From the composition data reported in Table 2, it may be observed that Mo content of the alloy is maximum for the coating developed at 1.0 A dm^{-2} (38.3%), and it decreased with an increase of c.d. It may be noted that an increase of c.d. from 1.0 to 4.0 A dm^{-2} resulted in the decrease of the Mo content to about 5 wt%. Regardless of the high Mo content in the bath (82.6%), wt% of Mo (38.3%) was found to be considerably less in the alloy coating. Thus, this unusual behaviour of small variation of Mo content, with c.d. may be attributed to the complexation of metal ions which affects the static potentials of the parent metals remarkably [22]. In other words, the bath exhibits very low partial current density for deposition of Mo (compared to its calculated limiting current density), due to a low rate of mass transport of electroactive species (Mo^{+2} ions) from a pH dependent molybdate-citrate complex. Hence, an unusual decrease of Mo content with c.d. is more due to change in pH (due to the evolution of H_2 gas), responsible for shifting of the equilibrium of its citrate complex, than due to change in its limiting current density [23]. This unusual change of composition with the c.d. is a distinctive nature of induced co-deposition of Ni-Mo alloy as observed by Bratoeva et al. [24]. The EDX spectrum showing the Ni and Mo content of Ni-Mo alloy deposited at 1.0 A dm^{-2} is shown in Fig. 5.

3.1.4. XRD study

XRD technique was used to determine the phase and crystallite size of the Ni-Mo alloy coatings at different c.d.'s. The characteristic XRD peaks of Ni-Mo alloys deposited at 1.0 A dm^{-2}–4.0 A dm^{-2} is presented in Fig. 6. The XRD peaks at 2θ = 22.3°, 43.3°, 50.4°, 74.03° and 89.8° represent tetragonal $MoNi_4$ phase [25], corresponding to the planes (110), (211), (130), (420) and (501), respectively, which is in good agreement with standard pattern of $MoNi_4$ (JCPDS no. 03-065-1533). A gradual increase in the intensity of peaks with c.d. clearly, indicates that deposition c.d. plays a significant role in structural property and composition of the coatings [17]. The grain size of the electroplated Ni-Mo alloy coatings, at different c.d., has been calculated

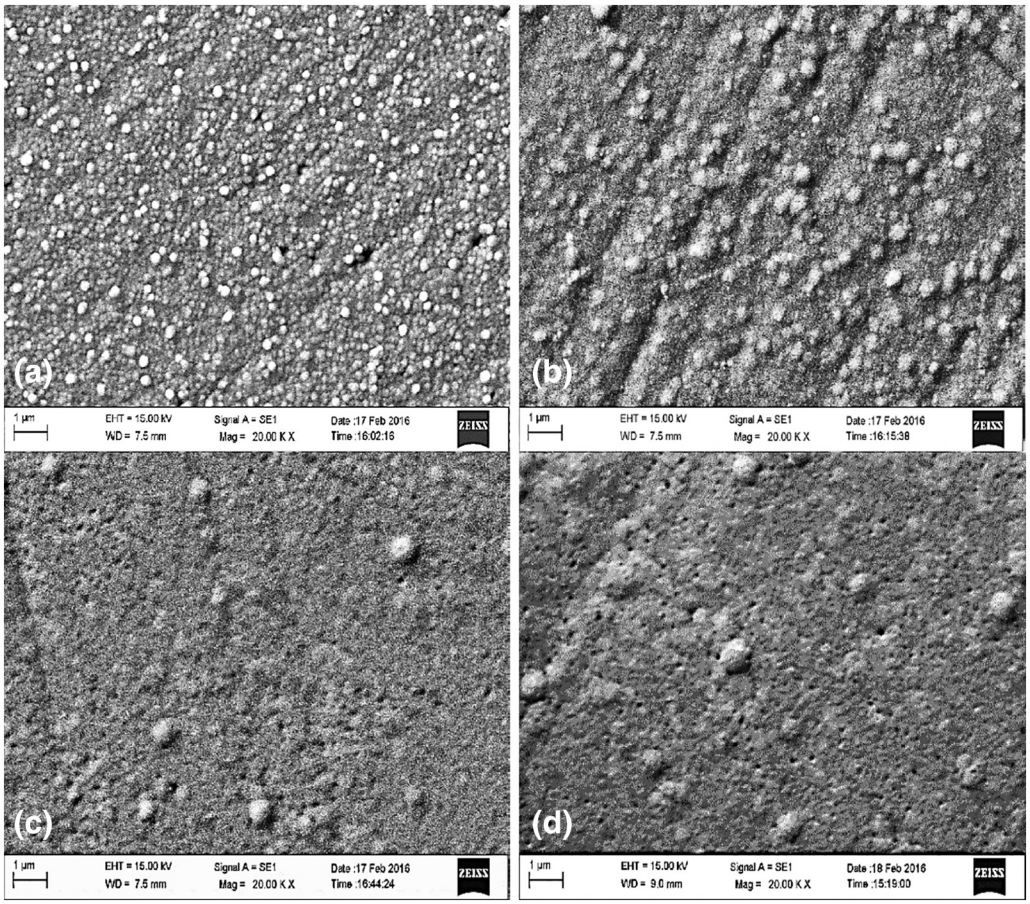

Fig. 3. SEM images of Ni-Mo alloy coating deposited at: a) 1.0 A dm^{-2}, b) 2.0 A dm^{-2}, c) 3.0 A dm^{-2} and d) 4.0 A dm^{-2}.

Table 2
Corrosion data, like E_{corr}, i_{corr} and CR of Ni-Mo alloy deposit at different c.d.

c.d. (A dm^{-2})	wt% Ni	wt% Mo	E_{corr} (V vs. RHE)	i_{corr} (µA cm^{-2})	CR × 10^{-2} (mm y^{-1})
1.0	61.7	38.3	0.724	26.90	25.27
2.0	64.3	35.7	0.707	25.08	23.76
3.0	65.6	34.4	0.690	22.12	21.06
4.0	66.8	33.2	0.685	20.85	19.94

using Scherrer equation [26],

$$d = \frac{0.9\lambda}{\beta \cos \theta} \quad (2)$$

here, d is the crystallite size, λ is the wavelength of X-ray radiation, β is the full width at half height of the diffraction peak and θ is the Bragg's angle. On calculating the average crystallite size of the coatings deposited over the wide range of c.d., was found to be 22.14 nm.

3.1.5. Potentiodynamic polarization study

To assess the stability of Ni-Mo alloy coatings as an effective material for water splitting applications, they have been subjected to

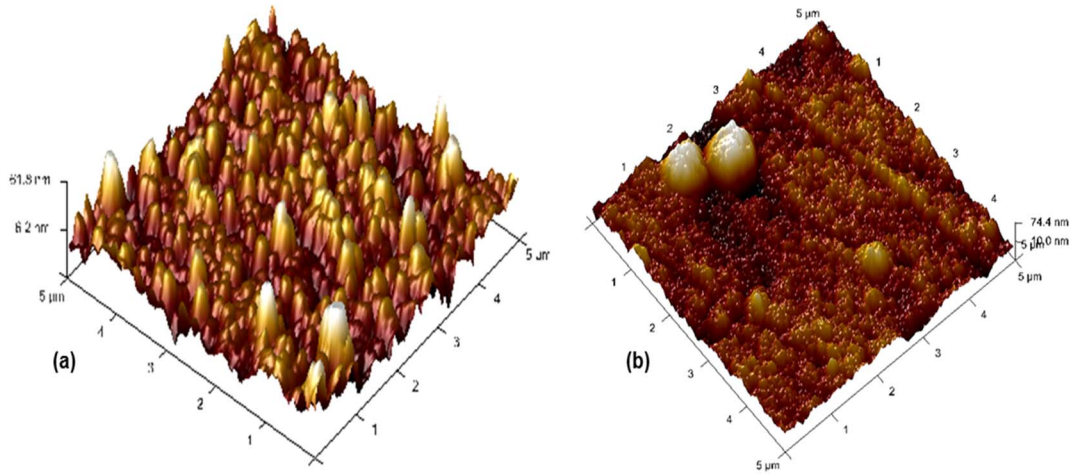

Fig. 4. Three-dimensional AFM image of Ni-Mo alloy coatings deposited at 1.0 A dm^{-2} (a), and 4.0 A dm^{-2} (b).

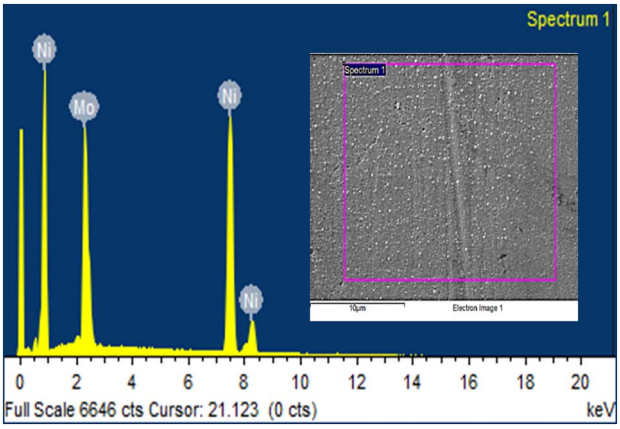

Fig. 5. EDX spectrum of Ni-Mo alloy coating showing the relative peaks corresponding to Ni and Mo content of the alloy deposited at 1.0 A dm^{-2}.

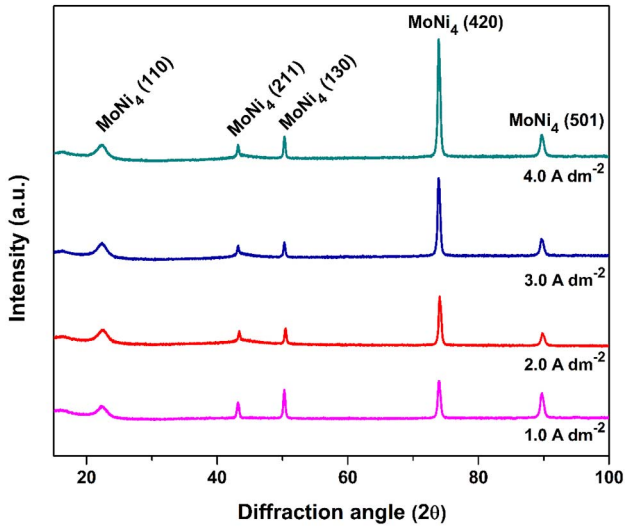

Fig. 6. X-ray diffractograms of Ni-Mo alloy deposit developed at different c.d.

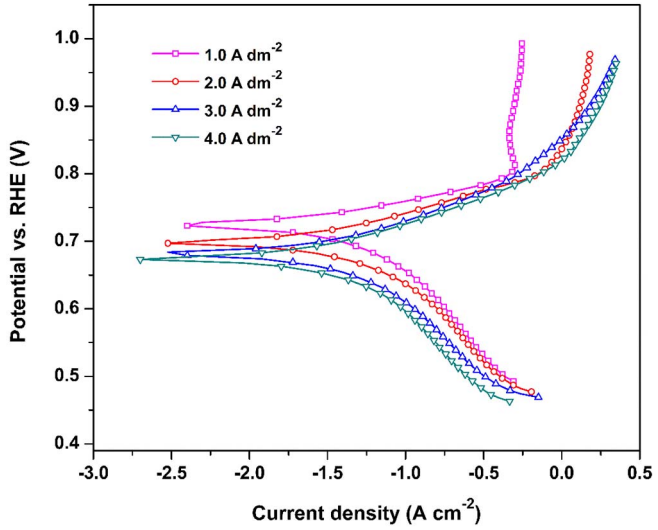

Fig. 7. Potentiodynamic polarization behaviour of Ni-Mo deposit developed at different c.d., using the same bath.

corrosion test in 1.0 M KOH (same medium in which water electrolysis is to be studied) by potentiodynamic polarization method [27]. The polarization behaviour of the coatings corresponding to different c.d. is shown in Fig. 7. The corrosion rates (CR) of Ni-Mo alloy coatings at different c.d. were estimated by Tafel extrapolation method and corresponding data are reported in Table 2. From the corrosion data, like E_{corr}, i_{corr}, β_c and CR reported in Table 2, it may be noted that the Ni-Mo alloy coating developed at 4.0 A dm^{-2} (having about 66.8% Ni) shows the least CR, i.e., 19.94 × 10^{-2} mm y^{-1}, while the coatings at lower c.d. are more susceptible to corrosion. Further, the decrease of CR at higher c.d. indicates that corrosion stability of the coatings is due to its high Ni content (refer Table 2). This decrease of CR towards high c.d. is due to increased smoothness, attributed by increased Ni content of the alloy, supported by SEM and AFM study, as discussed earlier.

Table 3
Kinetics parameters for the HER and OER on Ni-Mo electrode in 1.0 M KOH solution, obtained from the potentiodynamic polarization curves.

c.d. (A dm^{-2})	i_o (μA cm^{-2})	β_c (mV dec^{-1})	β_a (mV dec^{-1})
1.0	3.18	115	61
2.0	2.89	116	59
3.0	2.64	118	58
4.0	2.49	120	56

Further, the exchange current density (i_o) and cathodic Tafel slopes (β_c and β_a), corresponding to each c.d. have also been determined from their potentiodynamic polarization curves, and are reported in Table 3. The HER kinetic parameters, like i_o, β_c and β_a were deduced from the linear part of semi-logarithmic polarization plots. Apparent i_o values were derived by extrapolation of Tafel plots to zero current potential. The i_0 value for the HER is generally accepted as one of the most important parameters describing the kinetics of the electrochemical charge-transfer reaction at the particular metal-solution interface and is a measure of electrocatalytic activity of the cathode [28]. As seen from the data in Table 3, the value of β_c increased with deposition c.d. indicating that electrocatalytic behaviour of Ni-Mo alloy coating towards HER decreases with deposition c.d. In other words, Ni-Mo alloy at 4.0 A dm^{-2} is less favourable for HER. Similarly, the value of β_a is found to be decreased with deposition c.d. of an alloy. Further, it is important to note that the β_a for Ni-Mo alloy deposited at 4.0 A dm^{-2} is found to be 56 mV dec^{-1} which is on par with the value reported in the literature [29,30]. This testifies the fact that Ni-Mo alloy deposited at higher c.d. range is more favourable for OER.

3.2. Electrocatalytic study

The electrocatalytic behaviour of any materials can be evaluated on the basis of their ability to catalyse the HER and OER since they are the fundamental process involved in water electrolysis and fuel cell applications [31]. CV and CP techniques are considered to deliver a wealth of information with certain parameters that helps in evaluation of electrocatalytic property for water electrolysis. In the CV study, the hydrogen desorption peak area is considered as one of the primary parameters, as it depends on the active specific surface of the deposit; if the active specific surface is larger, the amount of hydrogen generated during the reduction of the adsorbed hydrogen on the electrode surface is higher. Onset potential is considered another important parameter characterizing the catalytic property of a cathodic material, determined by intercepting the voltammetric curve tangent to the potential axis [32]. In CP study, a constant current is applied to the counter and working electrodes, where the variation in potential of the working electrode is monitored. When the controlled amount of current is passed between the counter and working electrode, initially its potential changes significantly due to the build-up of charge at the electrode-solution interface until the potential is reached at which the electrolysis on the surface of electrode commences [33]. Hence Ni-Mo alloy coatings, deposited at different c.d. from the proposed bath have been subjected to series to tests to determine its electrocatalytic activity towards HER and OER in 1.0 M KOH medium, and the experimental

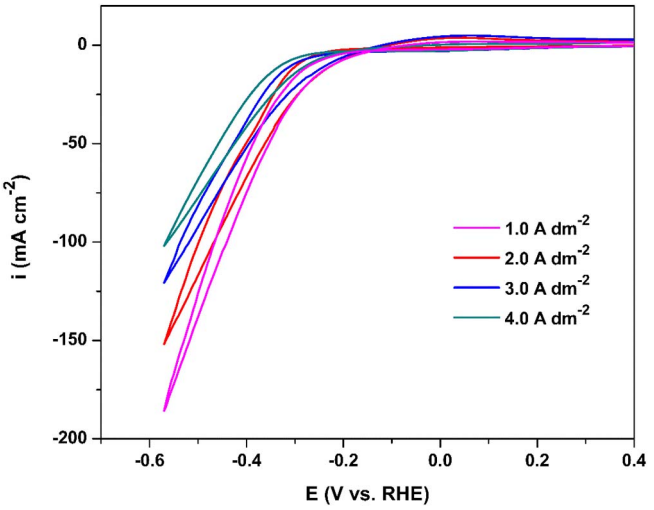

Fig. 8. Cyclic voltammograms of Ni-Mo alloy deposits developed at different c.d.'s with their cathodic peak current density, i_{pc} for HER.

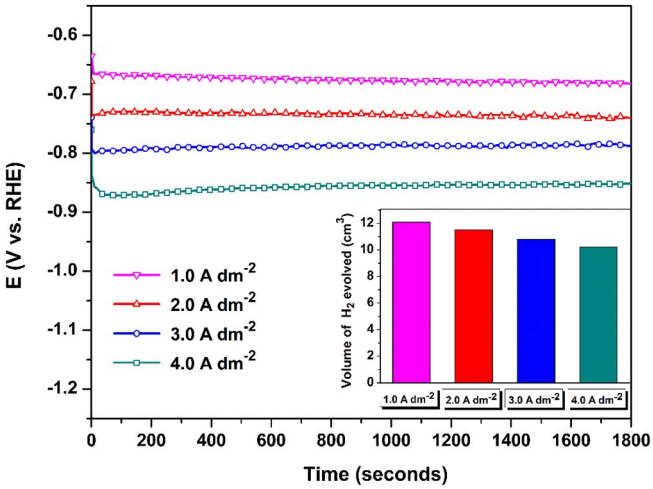

Fig. 9. Chronopotentiograms of Ni-Mo deposits, developed at different c.d. under impressed cathodic current of -300 mA cm^{-2} (volume of H_2 evolved in 300 s on each test electrodes are shown in the inset).

results are testified in the following sections.

3.2.1. Electrocatalytic behaviour for HER

3.2.1.1. Cyclic voltammetry study. CV is a powerful tool to provide substantial information on the thermodynamics of redox processes and the kinetics of heterogeneous electron-transfer reactions and of coupled chemical reactions or adsorption processes. Hence, CV study of Ni-Mo deposits developed at 1.0–4.0 A dm^{-2} for HER is made in the potential range of 1.03 V to -0.57 V, at 50 mV s^{-1} scan rate for 50 cycles. It was observed that the initial cycles showed larger cathodic *peak current density* (i_{pc}) values which eventually decreased with further increase in a number of cycles. Nearly after 25 cycles, the value of i_{pc} was found to remain constant, and CV curves were observed to retrace the previous cycle. This situation is corresponding to the condition where a rate of adsorption of H atom on the surface of an electrode for the formation of H_2 gas is equal to the rate of desorption of H_2 gas [34].

The cyclic voltammograms for HER of Ni-Mo alloy deposits, developed at different c.d. are shown collectively in Fig. 8, and corresponding electrochemical parameters were drawn are given in Table 4. From Fig. 8, it could be concluded that Ni-Mo alloy deposited at 1.0 A dm^{-2} exhibits the highest i_{pc} value (-0.186 A cm^{-2}) when compared to all other coatings.

The highest i_{pc} value recorded by the deposit at 1.0 A dm^{-2} may be ascribed to the highest Mo content (38.3 wt%) of the deposit when compared to other coatings. As the wt% of Mo content in the alloy is increased, the onset potential of an electrode for HER shifted in the positive direction favouring hydrogen generation with lower overpotential, a similar observation was reported by Manazoğlu, and co-workers [35]. Therefore, this particular coating at 1.0 A dm^{-2} showed the least onset potential and the least overpotential for HER reaction as reported in Table 4. Further, it is important to note that the onset potential for HER is -0.18 V (vs. RHE) for Ni-Mo alloy deposited at 1.0 A dm^{-2} is found to be on par with the values already reported in the literature [36,37]. It can be finally concluded that HER activity enhancement for Ni-Mo alloy coatings is due to a combination of increased surface area and increased fundamental catalytic activity [38].

Table 4
The HER parameters of Ni-Mo alloy deposits developed at different c.d. from the optimal bath.

c.d. (A dm^{-2})	Cathodic peak c.d. (i_{pc}) (A cm^{-2})	Over potential for HER (mV vs. RHE)	Onset potential for HER (V vs. RHE)	Volume of H_2 evolved 300 s (cm^3)
1.0	− 0.186	− 263.4	− 0.18	12.0
2.0	− 0.152	− 291.7	− 0.20	11.5
3.0	− 0.121	− 300.4	− 0.22	10.8
4.0	− 0.102	− 326.5	− 0.24	10.2

3.2.1.2. Chronopotentiometry study. The CP study on Ni-Mo alloy coatings, deposited at different c.d. (1.0–4.0 A dm^{-2}) to analyse their efficiency towards HER was determined by applying a constant current of -300 mA cm^{-2} for the duration 1800 s. The electro-catalytic activity of each Ni-Mo alloy deposits was assessed by measuring the volume of H_2 liberated for initial 300 s (Table 4). The chronopotentiograms obtained for each sample are shown in Fig. 9, with the volume of hydrogen gas collected (in the inset), and in Table 4.

Experimental results showed that alloy deposited at 1.0 A dm^{-2} produces a maximum amount of H_2, compared to the coatings deposited at higher c.d., concluding that it is electro-catalytically more active for HER. Further, an initial change of potential was observed in all samples soon after the initiation of electrolysis, followed by a steady-state potential response. This may be due to sudden exhaustion of the electrolysed components at the surface of the electrode, where H^+ ions from the solution undergo reduction to release H_2 gas, and ultimately a state of equilibrium is established between H^+ ions and H_2 during the process [17,34]. However, as the electrolysis further proceeds, almost a constant potential is achieved as observed in Fig. 9. During this stage, the evolution of hydrogen gas takes place uninterruptedly on the surface of an electrode, where the current applied is spent completely for conversion of H^+ ions into H_2 gas.

3.2.2. Electrocatalytic behaviour for OER

3.2.2.1. Cyclic voltammetry study. Fig. 10 shows the cyclic voltammograms recorded for Ni-Mo alloy coatings at 1.0, 2.0, 3.0 and 4.0 A dm^{-2} in the potential range of 1.03 to 1.78 V at a scan of 50 mV s^{-1}. The OER is believed to catalyse by the redox transitions of interfacial oxy-cations between higher and lower oxidation states [39,40]. Therefore, OER of Ni-Mo alloy coatings is attributed to electrochemical properties of redox pair just before the onset of oxygen evolution [41]. The onset potential of oxygen evolution was defined as the decomposition potential of water under the anodic polarization because the OER is an irreversible reaction with a high activation over potential [42].

The values for *anodic peak current density* (i_{pa}) and onset potentials derived from the graphs for OER are reported in Table 5. From the recorded electrochemical parameters, it may be noted that the Ni-Mo

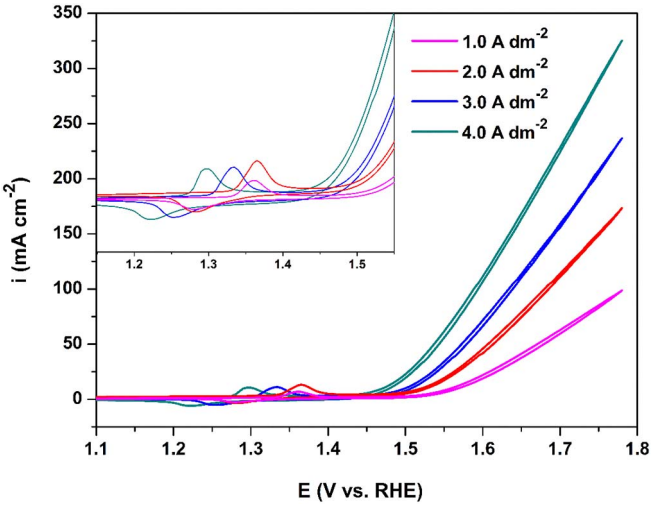

Fig. 10. The CV curves of Ni-Mo alloy coatings deposited at different c.d. demonstrating their anodic peak current density i_{pa} for OER, and their redox couples are shown in the inset.

Table 5
Electrode kinetic parameters of OER on the surface of Ni-Mo alloy coatings electrodeposited at different c.d.

c.d. (A dm^{-2})	Anodic peak c.d. (i_{pa}) (A cm^{-2})	Over potential for OER (mV vs. RHE)	Onset potential for OER (V vs. RHE)	Volume of O_2 evolved 300 s (cm^3)
1.0	0.098	155.9	1.50	8.1
2.0	0.173	152.1	1.48	8.7
3.0	0.237	150.0	1.46	9.5
4.0	0.325	147.2	1.42	10.3

alloy deposited at 4.0 A dm^{-2} presents good catalytic activity for OER with maximum i_{pa} of 0.325 A cm^{-2}, and least onset potential (1.46 V), compared to coatings at deposited at lower c.d.'s. Here, it is important to note from the nature of CV curves, both anodic peak i_{pa} and onset potentials of Ni-Mo alloy coatings has a strong dependency on the c.d. used. In other words, it depends directly on the Mo content of the alloy.

Oxygen evolution on the Ni-Mo coating deposited at 4.0 A dm^{-2} occurs at a less positive potential than on the alloy deposited at lower c.d. (1.42 V vs. RHE) which is on par with the value reported in the literature [43,17]. This further confirms that alloy coating at 4.0 A dm^{-2} shows improved OER activity than the rest [39]. The positive shift in redox potentials results in the fact that oxygen evolution commences immediately when the electrode potentials just reach the redox potential of this redox couple, probably indicating a better catalytic activity for the OER [42]. As it can be seen from Table 5, Ni-Mo alloy deposited at 4.0 A dm^{-2} exhibit the least over potential value of 147.2 mV, compared to coatings at another c.d. This points out the fact that, the deposit coated at higher c.d. is the most electrocatalytically active for OER.

3.2.2.2. Chronopotentiometry study. The CP technique has been employed to estimate the OER activity of Ni-Mo alloy coatings in the same medium, following CV study in a similar manner as HER analysis, with the quantity of O_2 liberated during the study was also measured. The chronopotentiograms for OER were recorded at a constant applied current of + 300 mA cm^{-2} (anodic) and the corresponding potential obtained were plotted against the time as shown in Fig. 11, with the volume of O_2, collected shown in the inset. Initially, during the beginning of the analysis, a sharp increase in the potential was observed, later this potential attains a stability, i.e., until when the potential for the formation of O_2 is reached (by the oxidation of OH^-).

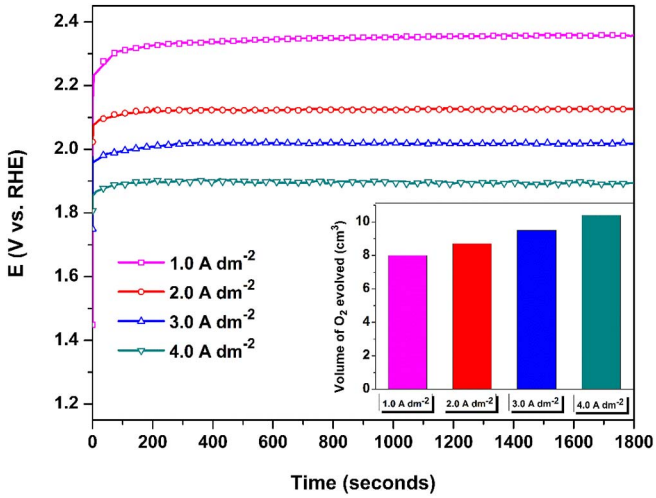

Fig. 11. Chronopotentiograms of Ni-Mo deposits developed at different c.d. under impressed anodic current of + 300 mA cm^{-2} (volumes of O_2 evolved in 300 s on each test electrodes are shown in the inset).

This stability is an equilibrium state associated with the newly forming oxygen bubble and bubbles escaping from the surface of the electrode [39,44].

Thus, from data obtained from i_{pc} and i_{pa} values, onset potentials, the amount of gases liberated and from their overpotentials (Tables 4 and 5), it may be concluded that electrodeposited Ni-Mo alloy developed at the lower c.d. (1.0 A dm^{-2}) is more suitable for HER and those at higher c.d. (4.0 A dm^{-2}) are best suitable for OER.

3.3. Mechanism of water splitting

To understand the mechanism of water electrolysis, on to the surface of present Ni-Mo alloy coatings and the factors responsible for favoured HER and OER under different conditions its composition, a well-known *spillover* process of heterogeneous catalysis has been proposed. It generally considers the synergism of transition metal-based alloys for water electrolysis [45]. Hence, it can be extended for Ni-Mo alloy coatings as well. According to this theory, a simple cooperative functioning of the alloy components is arbitrated via, rapid intra- and inter-particle surface diffusion of H ad-atoms. It is postulated that Ni sites on the Ni-Mo surface influence proton discharge, and serve as a hydrogen source for neighbouring Mo sites which act as hydrogen 'trap' sites where the ion/atom recombination of ad hydrogen atom to form hydrogen molecule and its desorption is promoted more efficiently. Highfield et al. [45] fundamentally ruled out any relationship between the electronic interactions among Ni-Mo alloy and observed synergy.

The electrocatalytic evolution of H_2 (HER) on the surface of Ni-Mo electrode surface can also be explained by the mechanism shown in Fig. 12(a). The HER in an alkaline solution is considered as an amalgamation of three basic steps, two electrochemical (Eqs. (3) and (4)) and one chemical (Eq. (5)).

$$M + H_2O + e^- \rightleftharpoons MH_{ads} + OH^- \quad \text{Volmer reaction} \tag{3}$$

$$MH_{ads} + H_2O + e^- \rightleftharpoons H_2 \uparrow + M + OH^- \quad \text{Heyrovsky reaction} \tag{4}$$

$$MH_{ads} + MH_{ads} \rightleftharpoons H_2 \uparrow + 2M, \quad \text{Tafel reaction} \tag{5}$$

It can be observed that the initial step is an electrochemical reduction of the water molecule, to give hydrogen adsorbed on the electrode surface by Volmer reaction (Eq. (3)), followed by Heyrovsky reaction (Eq. (4)), an electrochemical step for adsorbed hydrogen to produce H_2, and/or by chemical reaction i.e. Tafel reaction (Eq. (5)). Choquette et al. have reported that HER follows different mechanism based on the value of Tafel cathodic slope, β_c [46]. It has been described that Tafel slope in range 66 mV dec^{-1} corresponds to Heyrovsky-

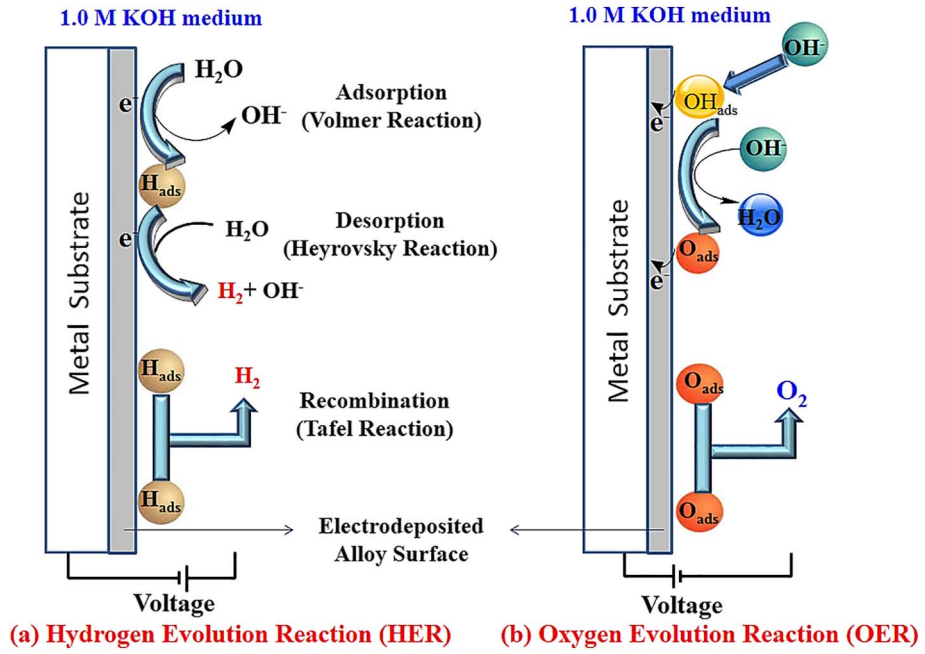

Fig. 12. The scheme representing the mechanism of HER and OER on the surface of Ni-Mo alloy coating of a specific composition when used as an electrode material, respectively in 1.0 M KOH solution.

Volmer mechanism, and in the neighbourhood of 118 mV dec^{-1} follows Volmer-Tafel mechanism, and finally above 200 mV dec^{-1} exhibit the Tafel mechanism. In the present study, it may be seen that β_c values of Ni-Mo alloy coatings deposited at increasing c.d. (determined from the linear part of Tafel plots, see Fig. 7) fall in the range of about 118 mV dec^{-1} as reported in Table 3. Hence, it may be inferred that Ni-Mo alloy coatings follow Volmer-Tafel type of mechanism for HER, and is shown schematically in Fig. 12(a).

Similarly, the OER proceeds in alkaline media via the steps sequentially shown below [47] and is shown schematically in Fig. 12(b)

$$OH^- \rightarrow (OH)_{ads} + e^- \quad (6)$$

$$(OH)_{ads} + OH^- \rightarrow (O^-)_{ads} + H_2O \quad (7)$$

$$(O^-)_{ads} \rightarrow (O)_{ads} + e^- \quad (8)$$

$$2(O)_{ads} \rightarrow O_2\uparrow \quad (9)$$

This behaviour could be described by the adsorption of relatively large OH^- ions on the surface of an electrode, where at the same time it overlaps with other processes like oxygen reduction reaction. Therefore, improved OER activity of Ni-Mo coating, developed at 4.0 A dm^{-2} can be ascribed to the increased adsorption of OH^- ions through the formation of a semiconducting layer in the range of applied potential [48]. Since the adsorption characteristics of the OH^- can lead to the formation of NiOOH on the electrode surface, the highest Ni content in the coating (66.8%), electrodeposited at 4.0 A dm^{-2} mainly favours the OER.

4. Conclusions

The following conclusions are established based on the systematic study on deposition, characterization and electrocatalytic study of the Ni-Mo alloy coating as electrode materials for alkaline HER and OER.

1. A Ni-Mo alloy bath has been optimized for the best performance of the coatings for water splitting applications (for both HER and OER) in 1.0 M KOH solution.
2. Experimental results revealed that Ni-Mo alloy electrodeposited at 1.0 A dm^{-2} (having 38.3 wt% Mo) and 4.0 A dm^{-2} (having 33.2 wt % Mo) shows better electrocatalytic property for both HER and OER, respectively, supported by CV and CP study.
3. Ni-Mo alloy coatings developed at 1.0 A dm^{-2} exhibit a maximum cathodic peak current density, $i_{pc} = -0.186$ A cm^{-2} at -1.57 V for HER and 4.0 A dm^{-2} shows maximum anodic peak current density, $i_{pa} = 0.325$ A cm^{-2} at 1.78 V for OER.
4. The highest electrocatalytic activity of Ni-Mo alloy coatings for both HER and OER, depending on deposition c.d. were attributed to their composition (in terms of wt% Ni and Mo), structure and surface morphology, supported by EDXA, XRD, SEM and AFM analyses.
5. Ni-Mo alloy coated at 4.0 A dm^{-2} is found to be more corrosion resistant in 1.0 M KOH medium, compared to coatings at another c.d.
6. The experimental study demonstrated that Ni-Mo alloy deposit follows the Volmer-Tafel type of mechanism for HER, supported by Tafel slope analyses.

Acknowledgements

The author, Sandhya Shetty is thankful to NITK, Surathkal, India for supporting this research in the form of Institute Research Fellowship.

References

[1] E. Navarro-Flores, Z. Chong, S. Omanovic, Characterization of Ni, NiMo, NiW and NiFe electroactive coatings as electrocatalysts for hydrogen evolution in an acidic medium, J. Mol. Catal. A Chem. 226 (2005) 179–197.
[2] C. Lupi, A. Dell'Era, M. Pasquali, Nickel–Cobalt electrodeposited alloys for hydrogen evolution in alkaline media, Int. J. Hydrog. Energy 34 (2009) 2101–2106.
[3] S. Trasatti, Work function, electronegativity, and electrochemical behaviour of metals: III. Electrolytic hydrogen evolution in acid solutions, J. Electroanal. Chem. 39 (1972) 163–184.
[4] H. Alemu, K. Jüttner, Characterization of the electrocatalytic properties of amorphous metals for oxygen and hydrogen evolution by impedance measurements, Electrochim. Acta 33 (1988) 1101–1109.
[5] J.-Y. Huot, L. Brossard, Cathodic behavior of amorphous Ni 0.33 Zr 0.67 alloy in 30 w/o KOH at 70 °C, Int. J. Hydrogen Energy 12 (1987) 599–605.
[6] D. Kreysa, B. Hajanson, Electrocatalysis by amorphous metals of hydrogen and oxygen evolution in alkaline solution, J. Electroanal. Chem. 201 (1986) 61–83.
[7] A. Budniok, J. Kupka, The evolution of oxygen on amorphous Ni-Co-P alloys, Electrochim. Acta 34 (1989) 871–873.
[8] R.E. Carbonio, V.A. Macagno, A.J. Arvía, The electrocatalytic activity of Ni (II)/Ni (III) oxide films in alkaline solutions, J. Electrochem. Soc. 147 (1983) 139–156.
[9] G.A. Snook, N.W. Duffy, A.G. Pandolfo, Evaluation of the effects of oxygen evolution on the capacity and cycle life of nickel hydroxide electrode materials, J.

Power Sources 168 (2007) 513–521.
[10] W. Li, X. He, J.N. Re, Ch. Jiang, Ch. Wan, Oxygen evolution improvement of Ni $(OH)_2$ by $Ca_3(PO_4)_2$ coating at elevated temperature, J. Electroanal. Chem. 597 (2006) 127–129.
[11] B. Chi, J. Li, X. Yang, Y. Gong, N. Wang, Deposition of Ni–Co by cyclic voltammetry method and its electrocatalytic properties for oxygen evolution reaction, Int. J. Hydrog. Energy 30 (2005) 29–34.
[12] K. Lian, S.J. Thorpe, D.W. Kirk, The electrocatalytic activity of amorphous and crystalline Ni-Co alloys on the oxygen evolution reaction, Electrochim. Acta 37 (1992) 169–175.
[13] P. Kedzierzawski, D. Oleszak, M. Janik-Czachor, Hydrogen evolution on hot and cold consolidated Ni–Mo alloys produced by mechanical alloying, Mater. Sci. Eng. A 300 (2001) 105–112.
[14] R. Schulz, J. Huot, M. Trudeau, Nanocrystalline Ni-Mo alloys and their application in electrocatalysis, J. Mater. Sci. 9 (1994) 2998–3008.
[15] I.A. Raj, V.K. Venkatesan, Characterization of Nickel-Molybdenum and Nickel-Molybdenum-Iron alloy coatings as cathodes for alkaline water electrolysers, Int. J. Hydrog. Energy 13 (1988) 215–223.
[16] E. Chassaing, M.P. Roumegas, M.F. Trichet, Electrodeposition of Ni-Mo alloys with pulse reverse potentials, J. Appl. Electrochem. 25 (1995) 667–670.
[17] Y. Ullal, A.C. Hegde, Electrodeposition and electro-catalytic study of nanocrystalline Ni–Fe alloy, Int. J. Hydrog. Energy 39 (2014) 10485–10492.
[18] N.V. Pardhasaradhy, Practical Electroplating Hand Book, New Jersey, Prentice Hall, 1987.
[19] M.G. Fontana, Corrosion Engineering, McGraw Hill, New York, 1987.
[20] A. Brenner, Electrodeposition of Alloys: Principles and Practice, Academic Press, New York, 1963.
[21] O. Aaboubi, Hydrogen evolution activity of Ni–Mo coating electrodeposited under magnetic field control, Int. J. Hydrog. Energy 36 (2011) 4702–4709.
[22] J. Halim, R. Abdel-Karim, S. El-Raghy, M. Nabil, A. Waheed, Electrodeposition and characterization of nanocrystalline Ni-Mo catalysts for hydrogen production, J. Nanomater. 2012 (2012) 1–9.
[23] C.G. Vayenas, R.E. White, M.E. Gamboa-Aldeco, Modern Aspects of Electrochemistry, Number 42, Springer, New York, 2008.
[24] M. Bratoeva, N. Atanasov, Effect of Sulfamate-Citrate electrolyte pH on the Ni-W alloy electrodeposition, J. Electrochem. 36 (2000) 60–63.
[25] J.M. Jaksic, M.V. Vojnovic, N.V. Krstajic, Kinetic analysis of hydrogen evolution at Ni–Mo alloy electrodes, Electrochim. Acta 45 (2000) 4151–4158.
[26] L. Anicaia, A. Petica, S. Costovici, P. Prioteasa, T. Visan, Electrodeposition of Sn and NiSn alloys coatings using choline chloride based ionic liquids–evaluation of corrosion behaviour, Electrochim. Acta 114 (2013) 868–877.
[27] D.A. Jones, Principles and Prevention of Corrosion, Prentice Hall, New Jersey, 1996.
[28] A.O. Yüce, A. Döner, G. Kardaş, NiMn composite electrodes as cathode material for hydrogen evolution reaction in alkaline solution, Int. J. Hydrog. Energy 38 (2013) 4466–4473.
[29] S.H. Ahn, A. Manthiram, Direct growth of ternary Ni–Fe–P porous nanorods onto nickel foam as a highly active, robust bi-functional electrocatalyst for overall water splitting, J. Mater. Chem. A 5 (2017) 2496–2503.
[30] X. Zhao, X. Shang, Y. Quan, B. Dong, G.Q. Han, X. Li, Y.R. Liu, Q. Chen, Y.M. Chai, C.G. Liu, Electrodeposition-solvothermal access to ternary mixed metal Ni-Co-Fe sulfides for highly efficient electrocatalytic water oxidation in alkaline media, Electrochim. Acta 230 (2017) 151–159.
[31] J. Kubisztal, A. Budniok, Study of the oxygen evolution reaction on nickel-based composite coatings in alkaline media, Int. J. Hydrog. Energy 33 (2008) 4488–4494.
[32] C. Lupi, A. Dell'Era, M. Pasquali, Nickel–Cobalt electrodeposited alloys for hydrogen evolution in alkaline media, Int. J. Hydrog. Energy 34 (2009) 2101–2106.
[33] I. Herraiz-Cardona, E. Ortega, J.G. Antón, V. Pérez-Herranz, Assessment of the roughness factor effect and the intrinsic catalytic activity for hydrogen evolution reaction on Ni-based electrodeposits, Int. J. Hydrog. Energy 36 (2011) 9428–9438.
[34] S.H. Ahn, S.J. Hwang, S.J. Yoo, I. Choi, H.-J. Kim, J.H. Jang, S.W. Nam, T.-H. Lim, T. Lim, S.-K. Kim, Electrodeposited Ni dendrites with high activity and durability for hydrogen evolution reaction in alkaline water electrolysis, J. Mater. Chem. 22 (2012) 15153–15159.
[35] M. Manazoğlu, G. Hapçı, G. Orhan, Effect of electrolysis parameters of Ni–Mo alloy on the electrocatalytic activity for hydrogen evaluation and their stability in alkali medium, J. Appl. Electrochem. 46 (2016) 191–204.
[36] L. Elias, A.C. Hegde, Modification of Ni–P alloy coatings for better hydrogen production by electrochemical dissolution and TiO_2 nanoparticles, RSC Adv. 6 (2016) 66204–66214.
[37] L. Yu, T. Lei, B. Nan, Y. Jiang, Y. He, C.T. Liu, Characteristics of a sintered porous Ni–Cu alloy cathode for hydrogen production in a potassium hydroxide solution, Energy 97 (2016) 498–505.
[38] J.R. McKone, B.F. Sadtler, C.A. Werlang, N.S. Lewis, H.B. Gray, Ni–Mo nanopowders for efficient electrochemical hydrogen evolution, ACS Catal. 3 (2013) 166–169.
[39] K.H. Kim, J.Y. Zheng, W. Shin, Y.S. Kang, Preparation of dendritic NiFe films by electrodeposition for oxygen evolution, RSC Adv. 2 (2012) 4759–4767.
[40] Y.S. Lee, C.C. Hu, T.C. Wen, Oxygen evolution on Co-Cu-Zn ternary spinel oxide-coated electrodes in alkaline solution integration of statistical, electrochemical, and textural approaches, J. Electrochem. Soc. 143 (1996) 1218–1225.
[41] C.C. Hu, Y.S. Lee, T.C. Wen, The physicochemical/electrochemical properties of binary Ni-Co oxides, Mater. Chem. Phys. 48 (1997) 246–254.
[42] C.C. Hu, Y.R. Wu, Bipolar performance of the electroplated iron–nickel deposits for water electrolysis, Mater. Chem. Phys. 82 (2003) 588–596.
[43] I. Elizabeth, A.K. Nair, B.P. Singh, S. Gopukumar, Multifunctional Ni-NiO-CNT composite as high performing free standing anode for Li ion batteries and advanced electro catalyst for oxygen evolution reaction, Electrochim. Acta 230 (2017) 98–105.
[44] A.P. Brown, M. Krumpelt, R.O. Loutfy, N.P. Yao, The effect of surface roughness on the hydrogen evolution reaction kinetics with mild steel and nickel cathodes, Electrochim. Acta 27 (1982) 557–560.
[45] J.G. Highfield, E. Claude, K. Oguro, Electrocatalytic synergism in Ni/Mo cathodes for hydrogen evolution in acid medium: a new model, Electrochim. Acta 44 (1999) 2805–2814.
[46] Y. Choquette, L. Brossard, A. Lasia, H. Menard, Study of the kinetics of hydrogen evolution reaction on Raney nickel composite-coated electrode by ac impedance technique, J. Electrochem. Soc. 137 (1990) 1723–1730.
[47] F. Chekin, H. Tahermansouri, M.R. Besharat, Nickel oxide nanoparticles prepared by gelatin and their application toward the oxygen evolution reaction, J. Solid State Electrochem. 18 (2014) 747–753.
[48] S. Shetty, A.C. Hegde, Electrodeposition of Sn-Ni alloy coatings for water-splitting application from alkaline medium, Metall. Mater. Trans. B Process Metall. Mater. Process. Sci. 48 (2016) 632–641.